IOP Conf. Series: Journal of Physics: Conf. Series **878** (2017) 012005 doi:10.1088/1742-6596/878/1/012005

Identified hadron production in pp collisions measured with ALICE.

Yasser Corrales Morales for the ALICE Collaboration
University and INFN of Turin, Via Pietro Giuria 1, 10125, Turin, Italy.
E-mail: corrales@to.infn.it

Abstract. The production of identified hadrons in proton-proton collisions is frequently studied as a reference for the investigation of the strongly-interacting medium created in heavy-ion collisions. In addition, at LHC energies measurements in pp and p–Pb collisions as a function of the event multiplicity have shown some features reminiscent of those related to collective effects in Pb–Pb collisions. Thanks to its excellent PID capabilities and p_{T} coverage, the ALICE detector offers a unique opportunity for the measurement of p_{T} spectra, integrated yields ($\mathrm{d}N/\mathrm{d}y$) and mean transverse momenta ($\langle p_{\mathrm{T}} \rangle$) of identified light-flavour hadrons at mid-rapidity over a wide p_{T} range.

In this contribution, results on π, K, p, $\mathrm{K}^0_{\mathrm{S}}$, Λ, Ξ, Ω and K^{*0} as a function of multiplicity in pp collisions at $\sqrt{s}$= 7 TeV are presented. The results are compared with those measured in p–Pb and Pb–Pb collisions. A similar evolution of the spectral shape, the p_{T}-differential particle ratios and the integrated yield ratios with the charged particle multiplicity in both small and large systems is observed. The production rates of strange hadrons in pp collisions increase more than those of non-strange particles, showing an enhancement pattern with multiplicity which is remarkably similar to the one measured in p-Pb collisions.

In addition, results on the production of light flavour hadrons in pp collisions at $\sqrt{s}$= 13 TeV, the highest centre-of-mass energy reached so far in the laboratory, are also presented and the behaviour observed as a function of $\sqrt{s}$ are discussed.

1. Introduction

Heavy ion collisions, such as Pb–Pb collisions at the Large Hadron Collider (LHC) at CERN, offer a unique possibility to study in the laboratory the properties of the strongly-interacting matter under extreme conditions of pressure, energy density and temperature. In particular, the deconfined quark-gluon plasma (QGP) system which is predicted by quantum chromodynamic (QCD) calculations can be investigated. The onset of this strongly interacting phase is accompanied by some peculiar signatures in the final state. These include the collective flow of particles created in the collision and an increase in the relative production rates of strange and multi-strange hadrons with respect to minimum-bias pp and p–Pb collisions.

The measurements performed in smaller systems (e.g systems created in pp and p–Pb collisions) provide the reference data for the interpretation of the nucleus-nucleus collision results. However, the analysis of the data samples of high multiplicity pp and p–Pb collisions collected during LHC Run-1, has surprisingly produced results qualitatively resembling the collective behaviour obtained in Pb–Pb collisions at LHC and Au-Au collisions at RHIC. Observations like long-range correlation structures in pseudo-rapidity observed in two-particle angular correlations [1, 2, 3, 4] and the hardening of the transverse momentum spectra of

identified particles [5] motivated several theoretical investigations [6, 7, 8, 9] as well as an effort on the experimental side in order to provide more comprehensive data from pp and p–Pb collisions. In this context, the study of identified hadrons as a function of the particle multiplicity in pp collisions allows to obtain better insight into the dynamics of small systems.

The ALICE apparatus [10] is well suited for the study of identified particles thanks to its moderate magnetic field, its high detector granularity and its excellent particle identification (PID) capabilities. In particular, PID is ensured over a wide transverse momentum range in the region at mid-rapidity via the measurement of specific energy loss in the Inner Tracking System (ITS) and in the Time Projection Chamber (TPC). Moreover, the particle velocity is measured via the Time Of Flight (TOF) detector, while the High Momentum Particle IDentification (HMPID) detector identifies particles by measuring the angle of emission of Cerenkov light emission.

2. Analysis Description

The measurements of pions, kaons and protons are performed combining the information from ITS, TPC, TOF and HMPID detectors [11]. Furthermore, a statistical PID method based on the relativistic rise of the $\mathrm{d}E/\mathrm{d}x$ in the TPC is applied to extend the measured p_{T} interval up to ≈ 20 GeV/c [12]. Strange ($\mathrm{K}^0_{\mathrm{S}}$, Λ, $\bar{\Lambda}$) and multi-strange hadron (Ξ^-, $\bar{\Xi}^+$, Ω^-, Ω^+) candidates are reconstructed via topological selection criteria and invariant mass analysis in the following channels (branching ratios): $\mathrm{K}^0_{\mathrm{S}} \to \pi\pi$ (69.2%), $\Lambda \to p\pi$ (63.9%), $\Xi \to \Lambda\pi$ (99.9%) and $\Omega \to \Lambda K$ (67.8%). The extraction of the raw yields were performed using the bin counting technique [13]. Finally, the production of short lived hadronic resonances (K^{*0}, $\bar{\mathrm{K}}^{*0}$) is also measured from the invariant-mass reconstruction of their decay products ($\mathrm{K}\pi$). The combinatorial background was estimated using a mixed-event technique and then subtracted from the original invariant-mass distribution. The raw yield is then extracted from a fit of the signal peak [14].

In all analyses, the transverse momentum spectra are corrected for acceptance and efficiency, which are determined through Monte Carlo simulations of the ALICE detector response. In addition, the measurement of light flavours hadrons concerns primary particles, i.e. particles produced either directly in the collision or formed by non-weak particle decays. Weak decays and contributions from particle knocked-out are removed with a data driven approach [15].

Multiplicity classes are defined on the basis of the total charge deposited in the V0A and V0C detectors located at forward ($2.8 < \eta < 5.1$) and backward ($3.7 < \eta < 1.7$) pseudo-rapidity regions, respectively. The mean pseudo-rapidity densities of primary charged particles $\langle \mathrm{d}N_{\mathrm{ch}}/\mathrm{d}\eta \rangle$ are measured at mid-rapidity, $|\eta| < 0.5$, for each event class [16]. In order to minimise spurious measurements originating from pile-up, events with more than one reconstructed primary vertex are rejected.

3. Results

The final transverse momentum spectra of the identified hadrons measured in pp collisions at $\sqrt{s} = 7$ TeV are reported in Fig. 1 for several event multiplicity classes, indicated by Roman numerals. The average charged particle densities in the highest (class I) and lowest (class X) multiplicity classes correspond to approximately 3.5 and 0.4 times the value in the integrated sample ($\langle \mathrm{d}N_{\mathrm{ch}}/\mathrm{d}\eta \rangle \approx 6.0$), respectively. For all the identified hadrons a clear hardening of the p_{T} spectra from low to high multiplicity events is observed. Moreover, this effect seems to be mass-dependent, being slightly more pronounced for the heavier particles. In fact, the baryon-to-meson ratio in pp collisions has been recently shown to follow a similar trend between lowest and highest multiplicity classes as the one observed in p–Pb and Pb–Pb collisions [5, 15]. In order to further explore the evolution of the different physics mechanisms related to baryon and meson production in different regions of the p_{T}-spectra, the ratio of proton-to-pion was studied at low-, mid- and high-p_{T} regions as a function of $\langle \mathrm{d}N_{\mathrm{ch}}/\mathrm{d}\eta \rangle$, as shown in Fig. 2. A continuity

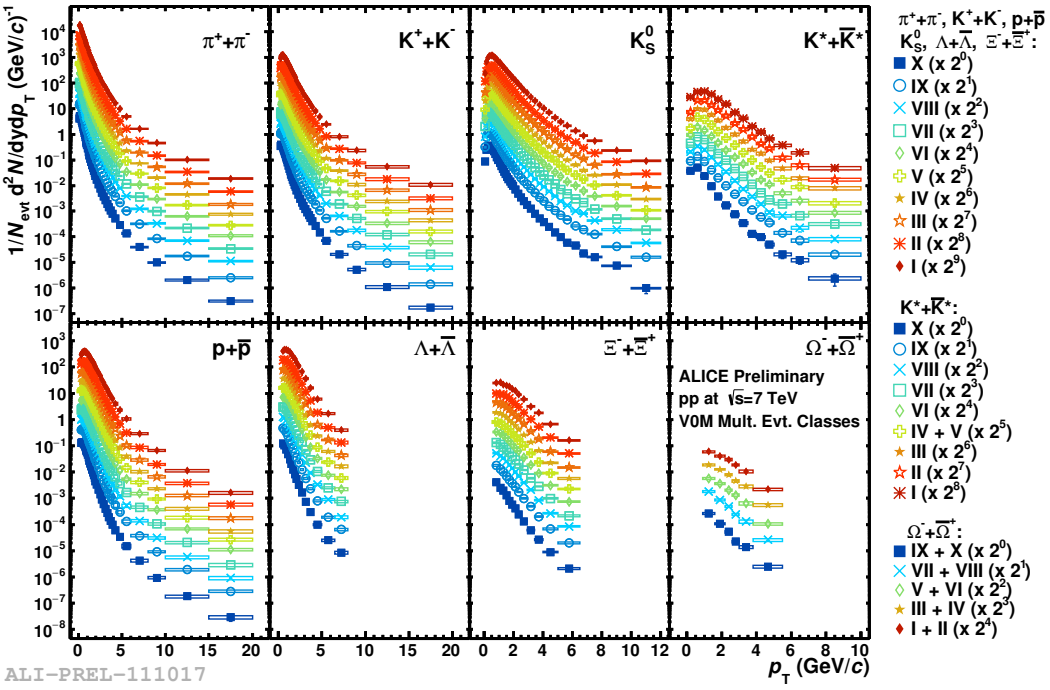

Figure 1. p_{T}-spectra of identified particles measured in pp collisions at $\sqrt{s}$= 7 TeV for several multiplicity classes, labelled by Roman numerals from high (class I) to low (class X) multiplicities.

across the various collision systems is observed for all the three p_{T} regions. The smooth evolution of the particle ratios suggests the similarity of the underlying mechanisms despite the differences in the initial colliding systems.

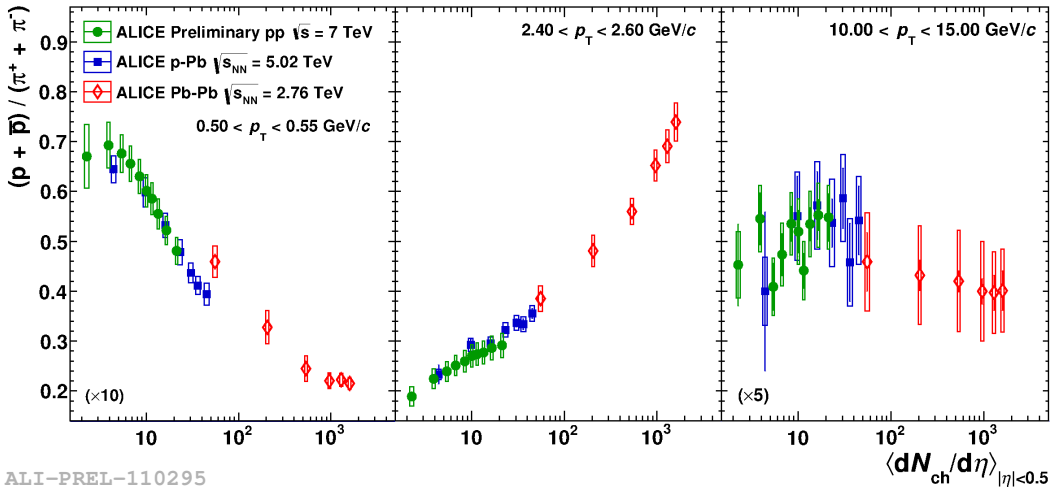

Figure 2. Proton–to–pion ratio at low (left panel), intermediate (middle panel) and high (right panel) transverse momentum as a function of the average charged particle density at mid-rapidity for pp, p–Pb and Pb–Pb collisions.

Comparisons with predictions from QCD-inspired models such as PYTHIA8 [17], DIPSY [18, 19, 20] and HERWIG7 [21, 22] have also been performed. The colour reconnection mechanism in PYTHIA8 as well as the colour ropes implementation in DIPSY seem to qualitatively reproduce the general trend observed at low and intermediate p_{T} (see Fig. 3). An alternative description is also provided by EPOS LHC [23], which implements collective radial flow using hydrodynamics. In this case, the predictions reproduce the data only qualitatively at low p_{T}.

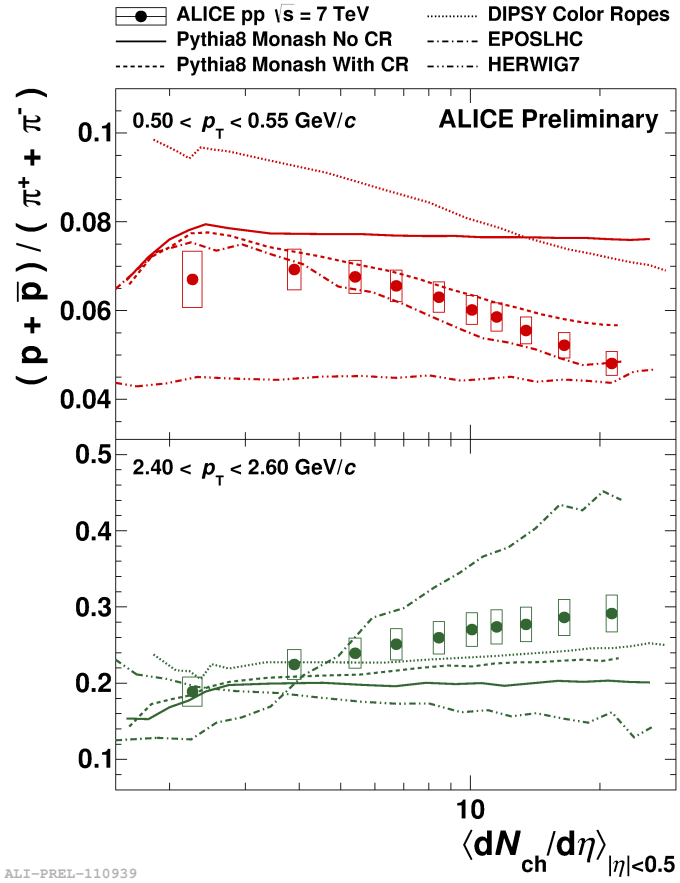

Figure 3. Proton-to-pion ratio at low (top panel) and intermediate (bottom panel) transverse momentum as a function of the average charged particle density at mid-rapidity for pp collisions at $\sqrt{s} = 7$ TeV (symbols) compared to model predictions (lines).

From the p_{T}-integrated yields of strange and multi-strange hadrons to pions, shown in Fig. 4 for pp, p–Pb and Pb–Pb collision systems, a multiplicity-dependent increase in the relative yield for particles having non-zero net strangeness content is observed. Moreover, the observed increase seems to dependent on the number of constituent strange quarks, as the increase in strangeness is larger for multi-strange hadrons. The comparison of the ratios with the predictions from Monte Carlo models shows that the increase is reproduced by the DIPSY event generator, while it is unable to reproduce the p/π ratio shown in Fig. 5. The EPOS model manages to describe only the magnitude of the effect and overestimates the rise while PYTHIA misses both trend and magnitude with increasing differences as the strangeness content increases.

The ratios between the p_{T}-integrated yields of particles with equal amount of strange valence quarks, such as $\Lambda/\mathrm{K}^0_{\mathrm{S}}$ and p/π, respectively, are reported in Fig. 5 as a function of the charged particle multiplicity for pp and p–Pb collisions. The trends for both ratios are independent of the event multiplicity, thus suggesting that the increase in the production of strange particles is related to the strangeness content rather than due to a difference in the particle masses. Comparisons to Monte Carlo models show poor agreement, especially when trying to reproduce all the observations simultaneously.

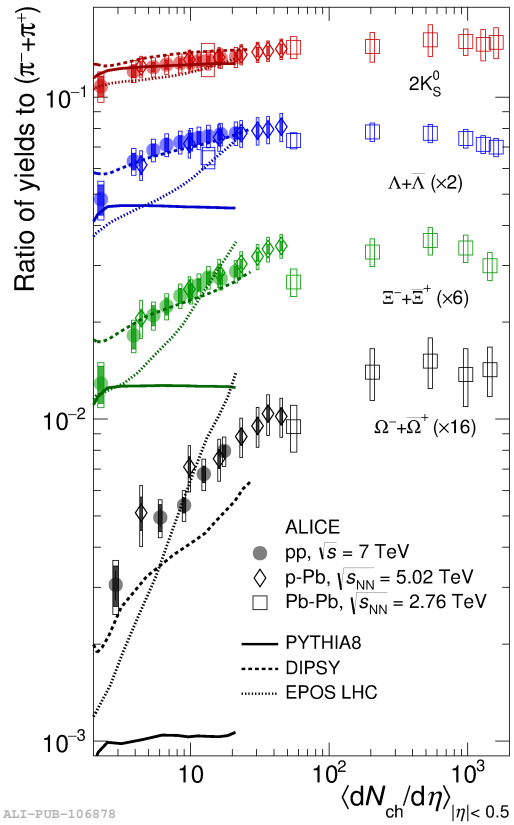

Figure 4. Ratios of K^0_S, Λ, Ξ and Ω yields to the one of π for pp, p–Pb and Pb–Pb collisions as a function of the charged multiplicity density compared to Monte Carlo models.

The evolution of particle ratios with the collision energy is another important aspect which may reveal essential details concerning the underlying particle production mechanisms. The p_T-integrated $(p+\bar{p})/(\pi^+ + \pi^-)$ and $(K^+ + K^-)/(\pi^+ + \pi^-)$ ratios measured by ALICE in pp collisions as a function of $\sqrt{s}$ are shown in Fig. 6. Results from E735 at $\sqrt{s} = 0.3$, 0.54, 1.0 and 1.8 TeV [25, 24], from PHENIX at $\sqrt{s} = 62.4$ and 200 GeV [26] and CMS at $\sqrt{s} = 0.9$, 2.76 and 7 TeV [27] are also shown and compared for both particle ratios. The results at 13 TeV confirms both the trend and the saturation behaviour observed at 900 GeV.

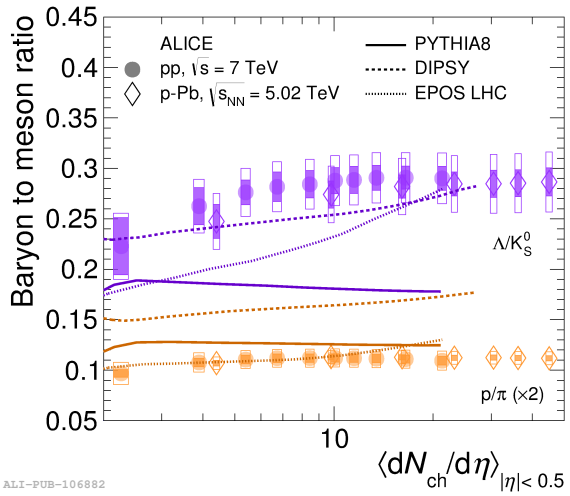

Figure 5. Λ/K^0_S and p/π ratios for pp and p–Pb as a function of multiplicity compared to Monte Carlo models.

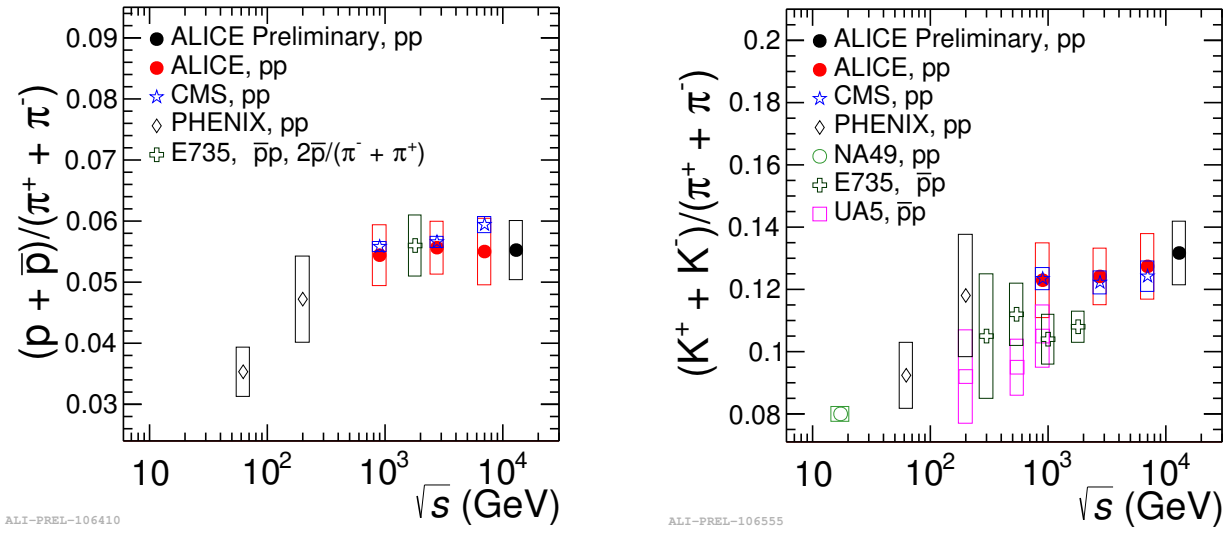

Figure 6. $(\mathrm{p}+\bar{\mathrm{p}})/(\pi^+ + \pi^-)$ and $(\mathrm{K}^+ + \mathrm{K}^-)/(\pi^+ + \pi^-)$ in pp and p$\bar{\mathrm{p}}$ collisions as a function of $\sqrt{s}$. ALICE measurements in pp collisions at $\sqrt{s}$ = 0.9, 2.76, 7 (red points) and 13 (black point) TeV are shown. Errors bars in ALICE results represent the quadratic sum of statistical and systematics uncertainties.

The hyperon-to-pion ratio as a function of $\sqrt{s}$ measured in ALICE is reported in Fig. 7. In comparison with the kaon- and proton-to-pion ratio the strange- and multi-strange-to-pion ratios show a hint of increase at 13 TeV with respect to the lower collision energies.

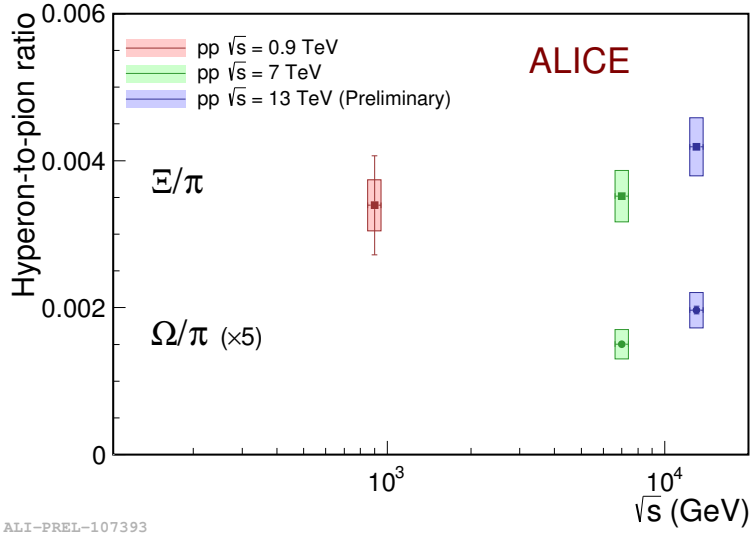

Figure 7. Hyperon to pion ratio in pp collisions as a function of the collision energy.

The K^{*0} and ϕ meson production has been also measured in pp collisions at $\sqrt{s}$ = 13 TeV. The p_{T}-integrated $\mathrm{K}^{*0}/\mathrm{K}$ and ϕ/K ratios are shown in Fig. 8. However, no energy evolution is observed in the range from RHIC to the highest LHC energy.

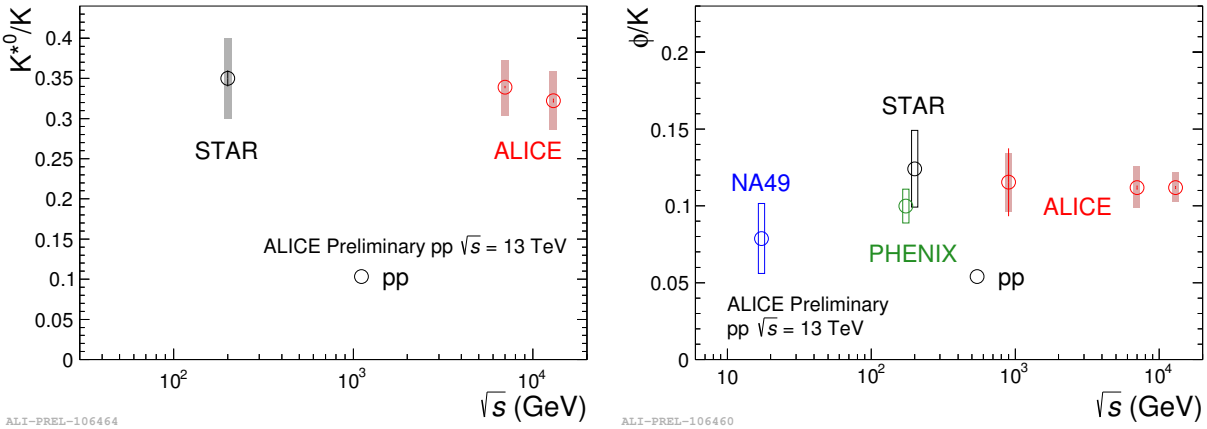

Figure 8. K^{*0}/K and ϕ/K ratio in pp collisions as a function of the collision energy. Bars represent statistical uncertainties. Boxes represent the total systematic uncertainties.

4. Summary and Outlook

The ALICE Collaboration has measured a comprehensive set of identified hadrons in pp collisions at $\sqrt{s} = 7$ TeV as a function of the charged particle multiplicity. A mass-dependent hardening of the spectral shapes was observed for high multiplicity collisions. In addition, a multiplicity-dependent increase in the production of strange hadrons relative to the production of pions was found. The effect seems to be related to the strangeness content rather than to the particle mass and it is qualitatively reproduced by Monte Carlo generators such as DIPSY, while the same model is not in quantitative agreement with the measurement for p/π.

We have also presented the measurement of the production of light flavour hadrons in pp collisions at 13 TeV, the highest centre-of-mass energy ever reached in the laboratory. Above $\sqrt{s} = 900$ GeV the $(p+\bar{p})/(\pi^+ + \pi^-)$ and $(K^+ + K^-)/(\pi^+ + \pi^-)$ ratios are energy independent within the systematic uncertainties. Furthermore, the hyperon-to-pion ratios at 13 TeV suggest an increase with respect the same results at lower energies. This effect may be related to the enhanced production of strange and multi-strange hadrons as a function of event multiplicity already observed in pp collisions at 7 TeV, as the mean charged particle multiplicity density also increases with collision energy [24]. Moreover, the relative production of strange resonances (K^{*0}/K and ϕ/K) remains constant within a wide range of centre of mass energies. Multiplicity dependent studies also in pp collisions at 13 TeV will help to disentangle the role of collision energy and event multiplicity in the particle production dynamics of pp collisions.

References

[1] CMS Collaboration, 2010 *JHEP* **09** 091 (*Preprint arXiv:1009.4122*)
[2] CMS Collaboration, 2013 *Phys. Lett. B* **718** 795
[3] ALICE Collaboration, 2013 *Phys. Lett. B* **719** 2941 (*Preprint arXiv:1212.2001*)
[4] ATLAS Collaboration, 2016 *Phys. Rev. Lett.* **116** 172301 (*Preprint arXiv:1509.04776*)
[5] ALICE Collaboration, 2014 *Phys. Lett. B* **728** 2538 (*Preprint arXiv:1307.6796*)
[6] Dusling K. and Venugopalan R., 2013 *Phys. Rev. D* **87** 094034 (*Preprint arXiv:1302.7018*)
[7] Ortiz Velasquez A. et al., 2013 *Phys. Rev. Lett.* **111** 042001 (*Preprint arXiv:1303.6326*)
[8] Bozek P. and Broniowski W., 2013 *Phys. Rev. C* **88** 014903 (*Preprint arXiv:1304.3044*)
[9] Ortiz Velasquez A. et al., 2016 *Preprint arXiv:1608.04784*
[10] ALICE Collaboration, 2008 *JINST* **3** S08002
[11] ALICE Collaboration, 2015 *Eur. Phys. J. C* **75** 226
[12] ALICE collaboration, 2011 *Eur. Phys. J. C* **71** 1594 (*Preprint arXiv:1012.3257*)
[13] ALICE Collaboration, 2016 *Preprint arXiv:1606.07424*
[14] ALICE Collaboration, 2012 *Eur. Phys. J. C* **72** 2183 (*Preprint arXiv:1208.5717*)

[15] ALICE Collaboration, 2012 *Phys. Rev. Lett.* **109** 252301
[16] ALICE Collaboration, 2013 *Phys. Rev. Lett.* **110** 032301 (*Preprint arXiv:1210.3615*)
[17] Sjostrand T., Mrenna S. and Skands P. Z. 2008, *Comput. Phys. Commun.* **178** 852867 (*Preprint arXiv:0710.3820*)
[18] Flensburg C., Gustafson G. and Lonnblad L., 2011 *JHEP* **08** 103 (*Preprint arXiv:1103.4321*)
[19] Bierlich C., Gustafson G., Lnnblad L. and Tarasov A., 2015 *JHEP* **03** 148 (*Preprint arXiv:1412.6259*)
[20] Bierlich C. and Christiansen J. R., 2015 *Phys. Rev. D* **92** 094010 (*Preprint arXiv:1507.02091*)
[21] Bahr M. et al., 2008 *Eur. Phys. J. C* **58** 639707 (*Preprint arXiv:0803.0883*)
[22] Bellm J. et al., 2016 *Eur. Phys. J. C* **76** 196 (*Preprint arXiv:1512.01178*)
[23] Pierog T. et al,. 2015 *Phys. Rev. C* **92** 034906 (*Preprint arXiv:1306.0121*)
[24] E735 Collaboration, 1992 *Phys.Rev. D* **46** 2773-2786.
[25] E735 Collaboration, 1993 *Phys.Rev. D* **48** 984-997.
[26] PHENIX Collaboration, 2011 *Phys. Rev. C* **83** 064903.
[27] CMS Collaboration, 2012 *Eur. Phys. J. C* **72** 2164.